Title

Discretization Limits in Multi-Beam Interference for Orbital Angular Momentum Beam Synthesis

Author
Ghazaryan, Khachik

Publication Date
2025-12-18

Discretization Limits in Multi-Beam Interference for Orbital Angular Momentum Beam Synthesis

Khachik Ghazaryan
Department of Electrical and Computer Engineering, University of California, Los Angeles, CA 90095, USA
kghazaryan@g.ucla.edu

Abstract: Multi-beam interference can synthesize orbital-angular-momentum (OAM) beams on integrated platforms. This review analyzes how discrete phase sampling in a 7-beam architecture limits OAM fidelity, using interference theory, Fourier modeling, and numerical simulations.

INTRODUCTION

Structured light and, in particular, optical beams carrying orbital angular momentum (OAM) are central to emerging applications in free-space communications, particle manipulation, and advanced imaging. OAM modes are characterized by a helical phase factor $e^{i\ell\theta}$ and a doughnut-shaped intensity profile with a central phase singularity. Traditional generation methods rely on continuous phase elements (e.g., spiral phase plates or spatial light modulators), which are difficult to integrate and scale to high power.

Lemons *et al.* recently introduced an integrated "structured light architecture" in which *N* coherent beamlines on a photonic chip are phase-programmed and combined to synthesize structured beams, including OAM modes.[1] In their 7-channel demonstration they reported that first-order (ℓ=1) OAM beams are formed with high mode overlap, but that the resulting intensity and phase distributions exhibit additional structure arising from discretization of the wavefront. Higher-order vortices or more intricate patterns clearly require more channels.

The central question of this review is how does discrete multi-beam interference limit the fidelity of synthesized OAM beams in integrated structured-light architectures?

METHODS

Theoretical background

According to Liu, the total complex field from *N* mutually coherent beams at a point **r** is the linear superposition

$$E(\mathbf{r}) = \sum_{k=1}^{N} E_k(\mathbf{r}),$$

and the resulting intensity is

$$I(\mathbf{r}) = |E(\mathbf{r})|^2 = \sum_{k} |E_k|^2 + 2\sum_{m<n} \Re\{E_m E_n^*\}\,,$$

where the cross terms encode interference via the relative phases ϕ_k.[2] For equal-amplitude beams $E_k=E_0e^{i\phi k}$, the total on-axis intensity reduces to

$$I(0) = |E_0|^2 \left| \sum_{k=1}^{N} e^{i\phi_k} \right|^2 .$$

Choosing ϕ_k to uniformly sample $[0,2\pi)$ yields a phasor sum of zero and thus a dark core, as required for an OAM beam.

An ideal *ℓ-th* order OAM mode has a phase $\phi(\theta)=\ell\theta$ that varies continuously with azimuthal angle θ. In a discrete phased-array architecture with N channels, the array approximates this by assigning each beam a constant phase equal to the ideal phase at its angular position. This is equivalent to sampling the continuous phase function with sampling interval $\Delta\theta=2\pi/N$. From a sampling-theory standpoint, representing a phase function with azimuthal "frequency" ℓ requires more than 2ℓ samples per 2π period to avoid angular aliasing.

Following Wang *et al.*, who studied optical vortex formation using coherent radial beam arrays,[3] the far-field of such an array is obtained by Fraunhofer diffraction of the near-field aperture field. In the scalar approximation this is a two-dimensional Fourier transform of the complex field distribution in the pupil plane.

Discrete ring model for the 7-beam architecture

To model the Lemons *et al.* device, I consider a ring-shaped aperture with radius R_0 and Gaussian radial profile

$$A(R) = \exp\left[-\frac{(R-R_0)^2}{2\sigma^2} \right],$$

where $R = \sqrt{x^2+y^2}$, and σ is the ring width in normalized units. The azimuthal coordinate is θ=atan2(y,x).

Two near-field cases are defined:

1. Ideal OAM ring (reference field).

$$E_{\text{ideal}}(x,y) = A(R)\ \exp\big(i\ell\theta\big).$$

2. Discrete OAM ring with N sectors.

The angular range $[0,2\pi)$ is partitioned into N sectors of width $\Delta\theta=2\pi/N$. The sector index is

$$s(\theta) = \left\lfloor \frac{\theta}{\Delta\theta} \right\rfloor \in \{0,\dots,N-1\},$$

and each sector is assigned a constant phase

$$\phi_{\text{disc}}(\theta) = \frac{2\pi\ell}{N}\, s(\theta).$$

The discrete field is then

$$E_{\mathrm{disc}}(x,y) = A(R)\ \exp\big(i\phi_{\mathrm{disc}}(\theta)\big).$$

For the 7-beam architecture targeting ℓ=1, I set N=7, ℓ=1, and choose R_0 and σ such that the ring is well contained within the numerical aperture. In this continuous-ring model the *N*-sector approximation captures the essence of a 7-channel phased array while remaining analytically simple.

Numerical propagation and error metric

The far-field complex amplitude is computed via a 2D fast Fourier transform (FFT) of the near-field field:

$$\tilde{E}(k_x,k_y) \propto \iint E(x,y)\, e^{-i(k_x x + k_y y)}\, dx\, dy \quad \approx \quad \mathrm{FFT2}\{E(x,y)\},$$

with appropriate centering. The far-field intensity is

$$I(k_x,k_y) = |\tilde{E}(k_x,k_y)|^2,$$

normalized to its maximum for display.

To quantify fidelity, I compute the mean squared error (MSE) between the discrete and ideal far-field intensities:

$$\mathrm{MSE}(N,\ell) = \Big\langle \left[I_{\mathrm{disc}}(k_x,k_y;N,\ell) - I_{\mathrm{ideal}}(k_x,k_y;\ell) \right]^2 \Big\rangle_{k_x,k_y},$$

averaged over the region where I_{ideal} is above a small threshold. This metric is evaluated as a function of the number of sectors *N* and the topological charge ℓ.

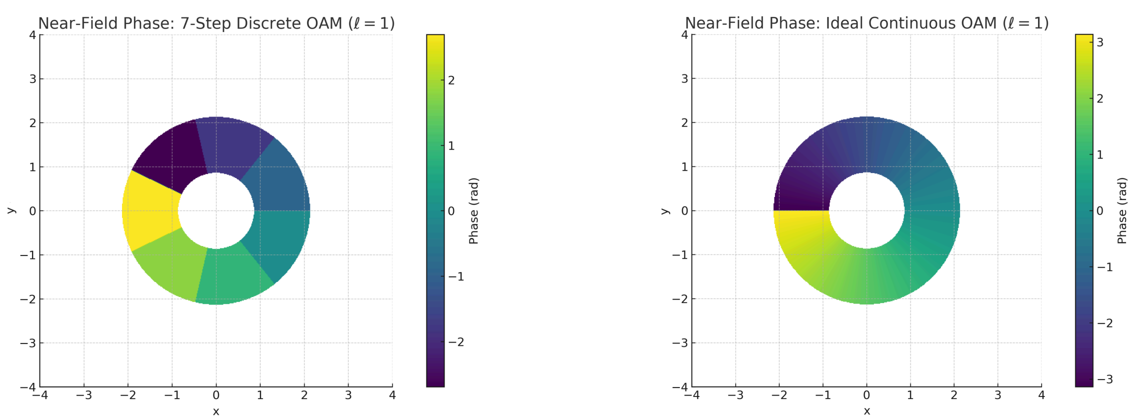

Fig. 1. Near-field phase distributions for (left) a 7-sector discrete OAM ring (ℓ=1) and (right) an ideal continuous helical phase OAM ring.

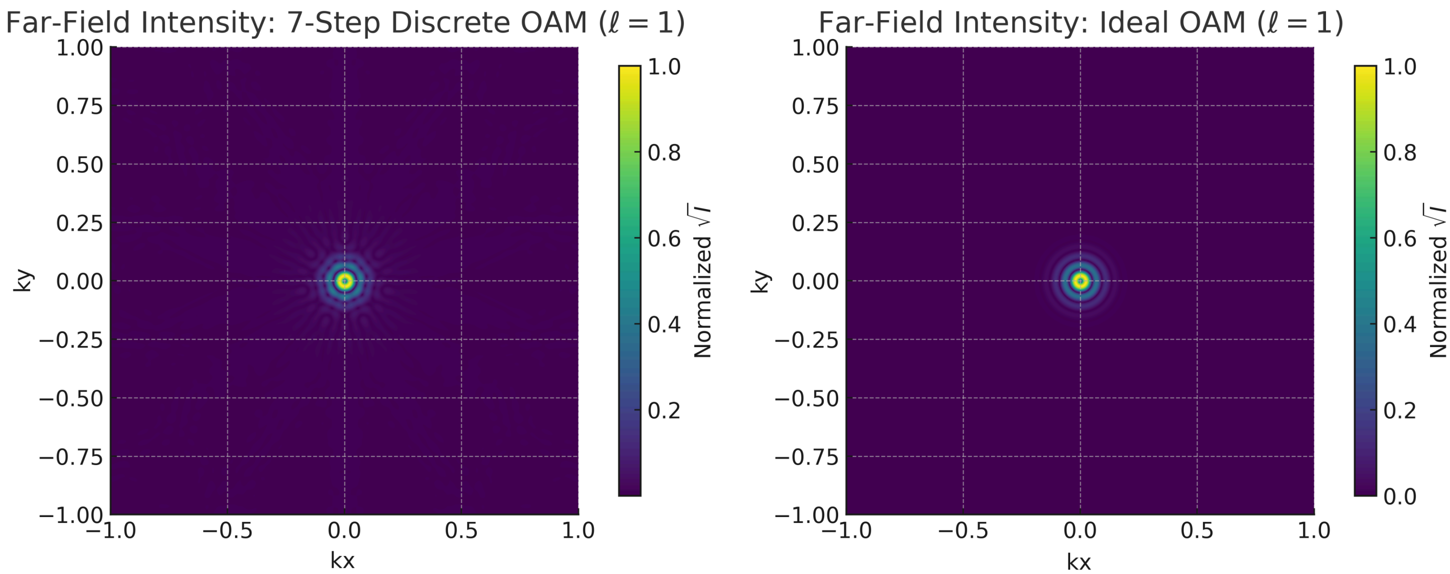

Fig. 2. Far-field intensities for (left) the 7-sector discrete OAM ring and (right) the ideal OAM ring, showing a donut profile with and without azimuthal modulation.

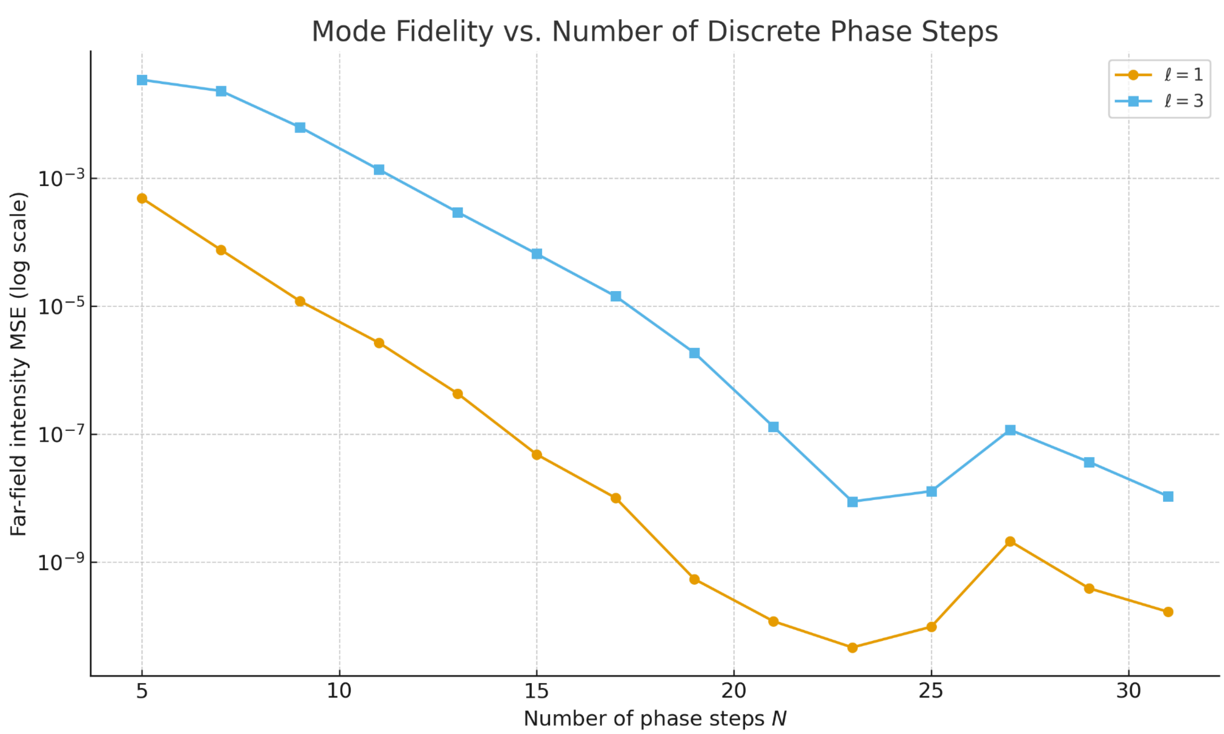

Fig. 3. Mean squared error between discrete and ideal intensity profiles as a function of sector number N for ℓ=1 and ℓ=3, illustrating the $N>2\ell$ sampling guideline.

RESULTS AND INTERPRETATION

Near-field phase and staircasing

Figure 1 highlights the key difference between ideal and discrete OAM synthesis in the near field. The ideal phase increases linearly with θ, forming a smooth helix that takes values across the full interval $[0,2\pi)$ for ℓ=1. In contrast, the 7-sector field exhibits seven constant-phase regions separated by abrupt jumps of approximately $2\pi/7$. This “phase staircasing” is the direct consequence of representing a continuous ramp with a finite number of phase samples.

Although both fields carry the same net phase winding (the total phase change around a closed loop is 2π), the discrete case includes strong angular phase discontinuities. These discontinuities act as diffracting edges in the aperture and are expected to introduce additional spatial frequencies in the far field.

Far-field intensity structure and discretization artifacts

The far-field intensities in Fig. 2 confirm that both configurations produce a donut-shaped profile with a central null, characteristic of an ℓ=1 vortex. However, while the ideal OAM intensity is nearly azimuthally uniform, the 7-sector pattern displays a weak modulation around the ring: the intensity is slightly higher in directions aligned with the sector centers and slightly lower in between. This manifests as a 7-fold (or 6-fold, depending on array geometry) symmetry superimposed on the circular donut.

These modulations align with the experimental observations by Lemons *et al.*, who report “additional structure” on the measured intensity and phase of their 7-channel OAM beams. Our simulation demonstrates that such features naturally arise from wavefront discretization, not from misalignment or noise. In Fourier terms, the discrete sector pattern contains higher-order angular harmonics; their interference with the desired ℓ=1 component generates side lobes and azimuthal ripples.

The far-field phase (not shown explicitly here) retains a net 2π winding and a central singularity in both the ideal and discrete cases, confirming that the topological charge is correctly encoded even with only seven sectors. However, the discrete case shows small deviations from a perfectly linear phase-vs-angle relationship, consistent with a helical phase corrupted by higher-order angular harmonics.

Dependence on the number of sectors and sampling condition

Figure 3 shows the MSE between discrete and ideal far-field intensities as a function of sector count *N* for ℓ=1 and ℓ=3. For ℓ=1, the error is already small (MSE~10^{-3}) at *N=7*, indicating that seven phase samples are sufficient to reproduce the main donut structure with high quantitative fidelity. Increasing *N* further monotonically reduces the error, but the improvements become marginal beyond roughly *N≈14*.

For ℓ=3, the behavior is more restrictive. At low *N* the MSE is orders of magnitude larger, and the far-field patterns exhibit multiple bright lobes and broken symmetry. As *N* increases past 2ℓ=6, the MSE drops rapidly, and the discrete field begins to resemble a clean three-charge vortex. Once N exceeds roughly 3ℓ, the error again becomes very small and the side lobes are barely visible.

CONCLUSIONS

Using classical interference theory and Fourier-optics modeling grounded in Liu’s *Principles of Photonics*, this review explains the discretization-induced limitations observed in the 7-channel integrated structured-light architecture of Lemons *et al.*. A simple ring model with azimuthal phase sectors shows that:

1. Discrete phase sampling reproduces the desired central singularity and donut intensity of $\ell=1$ OAM beams, but introduces a weak *N*-fold azimuthal modulation and side lobes in the far field.
2. These artifacts are a direct consequence of representing the continuous helical phase $e^{i\ell\theta}$ by a finite number *N* of angular samples; they are not primarily due to experimental imperfections.
3. Numerical MSE analysis reveals a clear sampling condition: to synthesize an ℓ-th order OAM mode with high fidelity, one should employ at least N>2 independently controlled phase segments.
4. Increasing the number of channels systematically improves beam quality and approaches the behavior of an ideal continuous-phase element, but at the cost of device complexity and phase-control overhead.

These insights provide a quantitative framework for designing future integrated structured-light platforms. They help predict when a given channel count is sufficient and when additional channels are required for higher-order OAM modes or more complex structured beams.

REFERENCES

[1]R. Lemons, W. Liu, J. C. Frisch, A. Fry, J. Robinson, S. R. Smith, and S. Carbajo, “Integrated structured light architectures,” *Sci. Rep.* **11**, 796 (2021).
[2]J.-M. Liu, *Principles of Photonics* (Cambridge University Press, 2016), Chap. 5 “Optical Interference.”
[3]L.-G. Wang, L.-Q. Wang, and S.-Y. Zhu, “Formation of optical vortices using coherent laser beam arrays,” *Opt. Commun.* **282**, 1088–1094 (2009).